

Electrochemical aptamer-based biosensor developed to monitor PSA and VEGF released by prostate cancer cells

Bruno P. Crulhas¹ · Agnieszka E. Karpik¹ · Flávia K. Delella¹ · Gustavo R. Castro¹ · Valber A. Pedrosa¹

Received: 3 August 2017 / Revised: 30 August 2017 / Accepted: 7 September 2017 / Published online: 14 October 2017
© Springer-Verlag GmbH Germany 2017

Abstract Early prostate cancer (PCa) diagnostic is crucial to enhance patient survival rates; besides, non-invasive platforms have been developed worldwide in order to precisely detect PCa biomarkers. Therefore, the aim of the present study is to develop a new aptamer-based biosensor through the self-assembling of thiolated aptamers for PSA and VEGF on the top of gold electrodes. This biosensor was tested in three prostate cell lines (RWPE-1, LNCaP and PC3). The results evidenced a stable and sensitive sensor presenting wide linear detection ranges (0.08–100 ng/mL for PSA and 0.15 ng–100 ng/mL for VEGF). Therefore, the aptasensor was able to detect the patterns of PSA and VEGF released *in vitro* by PCa cells, which gave new insights about the prostate cancer protein dynamics. Thus, it could be used as a non-invasive PCa clinical diagnosis instrument in the near future.

Keywords Aptasensor · Protein released by cancer cell · Biomarkers · *In vitro* experiments

Introduction

Prostate cancer (PCa) is becoming a disease of increasing significance worldwide. Estimates assume it as the second most common cancer type in men; accordingly to the American Cancer Society the projection for 2017 are 161,360 new cases of PCa with 26,730 death from PCa. Moreover, 1 man in 7 will be diagnosed with PCa during his

lifetime, which made the disease the fifth leading cause of death among men [1]. The mortality rates are annually increasing due to the difficulty of diagnosing the disease in its initial stages [2]. So far, the traditional clinical diagnostic techniques rely on transrectal ultrasonography, digital rectal examination (DRE), computed tomography scan, magnetic resonance imaging and cancer protein assay [3–6]; however, most of these techniques are invasive, require time and need to be performed by skilled professionals. It is crucial detecting and diagnosing PCa cases in their initial stages; therefore, the need of more powerful diagnostic instruments has been growing. Accordingly, the use of new biomarkers for PCa diagnostic has become a very specific and promising research field [7, 8].

The prostate-specific antigen (PSA) has been the most popular and effective marker used to detect PCa since 1994 [9]. Clinical data have shown that values of PSA higher than 4 ng/mL are treated as abnormal [10]; however, PSA itself lacks specificity to precisely detect the presence of PCa. High PSA levels can be related to benign prostatic hyperplasia (BPH), prostatitis, or cystitis [11–13]. Due to lack of accuracy, other proteins such as the vascular endothelial growth factor (VEGF) have been investigated as additional biomarker to improve PCa-detection efficiency [14].

The VEGF is a protein from the platelet-derived growth factor family of cystine-knot growth factors, and it is mainly responsible for stimulating vasculogenesis and angiogenesis. Moreover, it plays a vital role in physiological functions such as bone formation and wound healing [15, 16]. The VEGF concentration monitoring may be adopted to detect diseases such as bronchial asthma and diabetes mellitus [17]; therefore, VEGF can be also used as biomarker to detect different human cancer types, including brain, lung, breast, urinary tract or gastrointestinal tumors due to its increased production [18–20]. Circulating levels of VEGF is a biomarker of the degree and activity of tumor angiogenesis and could improve

✉ Valber A. Pedrosa
vpedrosa@ibb.unesp.br

¹ Department of Chemistry and Biochemistry, Institute of Bioscience, UNESP-Botucatu, Distrito de Rubiao Jr, 18618-000 Botucatu, São Paulo 18618-000, Brazil

PSA diagnosis accuracy for PCa [14]. However, only few systems were able to detect VEGF and PSA proteins simultaneously; however, they are often based on ELISA, fluorescence or electrochemical techniques and are dependent on the quality of antibodies for their sensitivity, specificity, moreover, they have the drawback of being relatively time consuming, and expensive which limits their applications [21]. Monitoring the VEGF and PSA concentration release by prostate cells is a suitable instrument to estimate cancer stage and it can provide an accurate diagnosis through non-invasive techniques.

Recent advances in the preparation of aptamers have promoted their usage in place of classical techniques due to their comparable binding affinities and stability under heat or pH variation. In addition, aptamers can be easily synthesized, isolated, and modified, and are highly resistant to denaturation [22, 23]. The probes are selected *in vitro* through exponential enrichment (SELEX) based on the ligands' systematic evolution [24]; more specific the selection of aptamers to target specific types of cells are nominated as Cell-SELEX [25]. The aptamer-based methods present countless advantages over the traditional antibody assays in early cancer detection; their main merits lie on high selectivity, affinity and stability. In addition, aptamers are cheaper than antibodies, they can also be regenerate after denaturation, which can increase the shelf life of a commercial aptamer-based detection kit developed for PCa diagnostic [26].

To better understand VEGF presence combined with PSA level as a prognostic factor for cancer detection, we described a novel electrochemical aptamer-based biosensor able to detect the VEGF and PSA released by prostate cancer cells in order to provide new insights about the PCa-stage evaluation and the protein release dynamics correlated to cancer aggressiveness which can be correlated with PSA and VEGF in serum for a more precise and cohesive diagnosis. The biosensor was based on the self-assembly of thiolated aptamers on gold-covered surface using methylene blue (MB) as redox label. When the protein binds to the aptamer, the DNA hairpin unfolds and it leads to electron transfer reduction and, consequently, to changes in the redox current. Our biosensor can be adopted to achieve a fast and accurate clinical PCa-stage diagnosis in the future.

Materials and methods

Chemicals and reagents

The silicon wafers (100 mm diameter, and 500 μm thick) were supplied by University Wafer (Boston, MA). The phosphate-buffered saline (PBS), 6-mercaptop-1-hexanol

(MCH), bovine serum albumin (BSA) (98%), uric acid (UA), ascorbic acid (AA), sulfuric acid (H_2SO_4), Ferrocene (Fc), Nucleopore Track-Etch Membrane (13 mm, 0.2 μm), prostate-specific antigen from human semen (99%) and human vascular endothelial growth factor were purchased at Sigma-Aldrich (St. Louis, MO). The Trypsin-EDTA, the cell culture medium RPMI 1640 (1 \times , with L-glutamine; VWR) supplemented with fetal bovine serum (FBS), the L-glutamine and the penicillin/streptomycin were purchased at Gibco®, (Waltham, MA). The aptamer sequences were used as follows:

PSA: 5'-SH/-TT TTT AAT TAA AGC TCG CCA TCA
AAT AGC TGG GGG-3'/MB
VEGF: 5'-SH/-T GTG GGG GTG GAC GGG CCG
GGT AGA-3'/MB.

Both were bought at Biosearch Technologies, Novato, CA, USA. Aptamer structures were analyzed by IDT OligoAnalyzer platform and it is possible to see the hairpin structure for both sequences (Scheme 1b.)

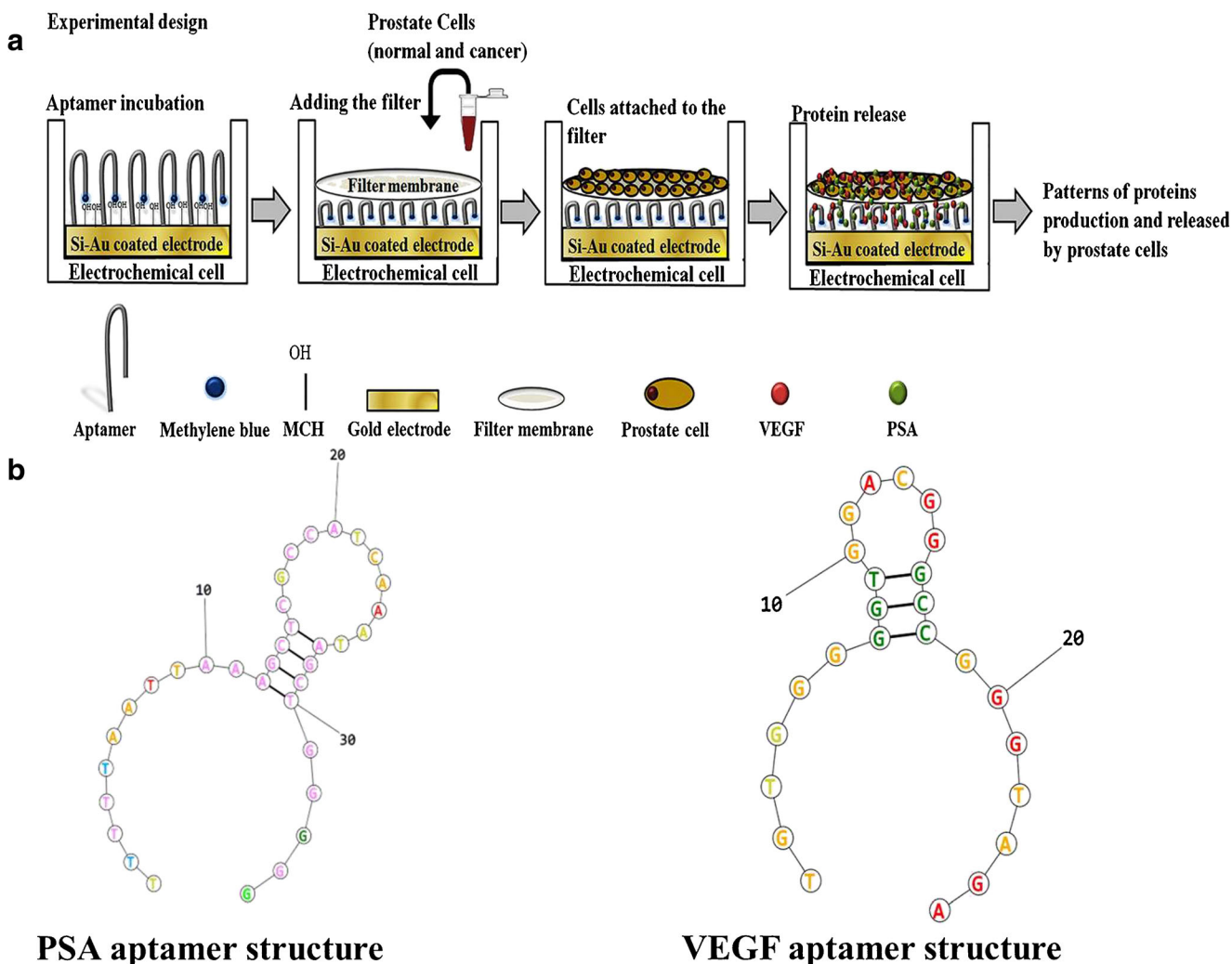
Gold-coated silicon electrode preparation

The silicon wafer worked as electrode in all electrochemical measurements; thus, it was modified at São Paulo University by the sputtering of a 5-nm gold layer and used as aptamers-attachment substrate. The aptamer was cleaned in isopropyl ethanol, rinsed in ultra-pure water and dried under nitrogen blowing, before its incubation in PSA or VEGF.

Preparing the aptamer-based biosensors

The aptamers were modified through Biosearch Technologies at 5'-terminus in C6-disulfide linker in order to have it bound to the gold electrode; and at 3'-end in MB (as redox probe) to perform the electrochemical analysis, which was followed by the HPLC purification process to remove truncated-synthesis products and to enrich the purity of the aptamer sequences. The VEGF and PSA aptamers stock solutions were diluted in 10 mM of PBS buffer (pH 7.4), according to the manufacturer's protocol.

Aptamer immobilization was conducted through the incubation of 1 μM thiolated aptamer on the top of the gold-coated silicon electrode for 18 h, in the dark, at 4 $^\circ\text{C}$. Subsequently, the electrodes were washed in ultra-pure water and immersed in 3 mM of MCH aqueous solution for 30 min. It was done to displace the nonspecifically adsorbed aptamer molecules and to passivate the electrode surface through the backfilling method. Finally, the electrodes were once more rinsed in DI water to remove MCH excesses; then they were ready to be immediately used in electrochemical measurements or to be stored in buffer solution at 4 $^\circ\text{C}$.



Scheme 1 a Overview of the experimental design applied to the aptamer-based electrochemical sensor self-assembled on the thiolated hairpin structure. A filter membrane was added on top of working electrode to provide the cell-attachment surface after aptamer incubation,

without compromising the aptamer layer. The pore membrane allowed target proteins to pass to the aptamer surface; the MCH backfilling avoided unspecific protein binding to the gold electrode surface. **b** PSA and VEGF aptamer structures

Prostate cell culture

The following cell lines were used: normal human prostate cells (RWPE-1; ATCC® CRL-11™), androgen-sensitive human prostate cancer cells (LNCaP; ATCC® CRL-1740™) and androgen-independent human prostate cancer cells (PC-3; ATCC® CRL-1435™). The three lineages (one composed by normal and two composed by tumor cells) were chosen to improve PSA and VEGF production comparisons and their release by a range of prostate cell types. Thus, the cells were cultivated in 75 cm² flasks containing RPMI media, supplemented with FBS, L-glutamine and penicillin/streptomycin. The cells were cultivated until they reached 90% confluence, after they were trypsinized in trypsin-EDTA. Cell viability was assessed through the Neubauer chamber technique; approximately 10⁵ cells were used in all experiments. A nuclear track-etch membrane with pore size 0.2 μm (Sigma-

Aldrich, St. Louis, MO) was used as cell-attachment surface, and it did not compromise the aptamer layer (Scheme 1).

Electrochemical characterization of the aptasensor

The aptasensor was characterized through scanning electron microscopy (SEM) using a Quanta 200 (FEI Company) coupled to an energy-dispersive X-ray spectroscopy analyzer (EDS) to make sure about the presence of the gold layer on the top of the silicon wafers.

The electrochemical characterization was conducted in a potentiostat μAutolabIII /FRA2 (Metrohm, NL), using a three-electrode system, which consisted of Ag/AgCl (3 M KCl), as reference electrode; Pt wire, as counter electrode; and gold-coated silicon wafer, as working electrode. The electrochemical characterization experiments were performed by cyclic voltammetry (CV) at scan rate 50 mV/s,

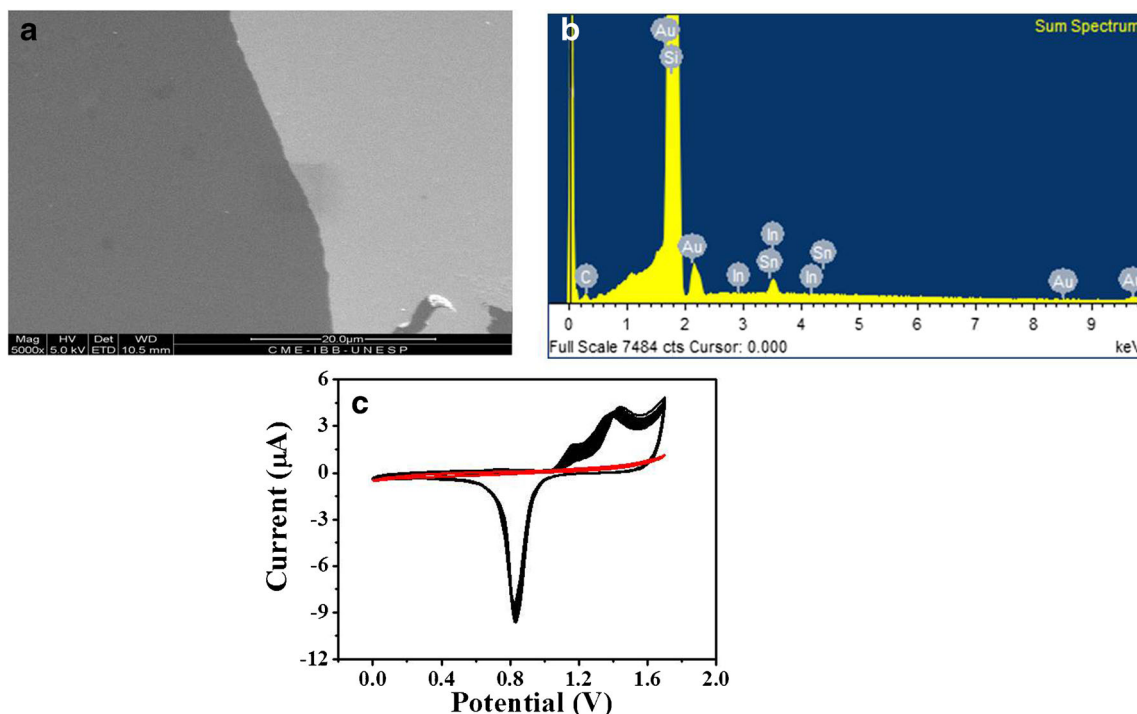


Fig. 1 **a** Scanning electron microscopy (SEM) of the gold-coated silicon wafer. **b** X-ray spectroscopy analysis (EDS) of the gold-coated silicon wafer. Black rectangle in the center represents the area selected for EDS

scan. **c** Cyclic voltammogram of bare silicon electrode (black dots) and gold-coated silicon electrode (black line) at potential range -0.2 to 1.5 V, and at 50 mV/s scan rate in 10 mM PBS buffer (pH 7.4)

ranging from -0.2 to 1.7 V, versus Ag/AgCl references in 1 mM H_2SO_4 (pH 7.4), 25 cycles of CV were done to evaluate the consistency of gold layer deposited on top of Si wafers. In addition to CV, electrochemical impedance spectroscopy (EIS) were done in order to validate the step by step assembling of the aptasensor by evaluation of charger transfer resistance with an amplitude of 0.005 V in frequency range of 0.001 to $10,000$ Hz in a 1 -mM H_2SO_4 solution (N_2 was bubbled for 10 min to remove O_2 from solution) containing 0.5 mM of Fc (pH 7.2), all impedance spectra were fitted to equivalent electrical circuits using NOVA software (Metrohm, NL).

Surface plasmon resonance (SPR) were done to evaluate the interaction between hairpin thiolated aptamer and gold surface regarding to the aptamer density over the Au surface (AutoLabSpringle, Eco Chemie, NL), in which an increase in the plasmon resonance angle of 120 millidegrees corresponds to a deposition of 1 ng/mm² on top of the gold disc, the experimental setup is described in details elsewhere [27].

PSA and VEGF electrochemical characterization and detection

The detection strategy relied on binding specific proteins to a self-assembled thiolated aptamer hairpin sensor in order to unfold hairpin structures, which decreased the efficiency of

electron transfer from MB to working electrode surface. Moreover, signal difference was measured through square wave voltammetry (SWV) at 40 mV amplitude, and 60 Hz frequency ranging from 0.0 to -0.5 V. The electrochemical cells consisted of multi-chamber batch mode with PSA or VEGF aptamer incubated separately and due to the fast SWV procedure it was able to do measurements with minimum time difference (less than 1 min).

The electrodes were modified by the aptamer molecules (PSA or VEGF), as described above, and were placed into custom-made Nylon electrochemical cells, in a system containing three electrodes. The aptasensor was allowed to equilibrate through stable faradaic current, in order to enable PSA and VEGF characterization and detection. Electrodes were characterized through SWV, without the presence of cells, to make sure that a well-formed aptamer layer would be formed; therefore, the electrode linked to the aptamers was stored in PBS buffer, only. Measurements were taken every 15 min, for 2 h, in order to evaluate changes in the aptasensor's background signal.

The VEGF and PSA aptamers were challenged in several concentrations of prostate specific antigen and human vascular endothelial growth factor, respectively, in the calibration curve analysis (PSA or VEGF aliquots of known concentration were introduced into the electrochemical cell after the background current stabilized). The sensor was allowed to react with analyte, for 20 min, before each measurement;

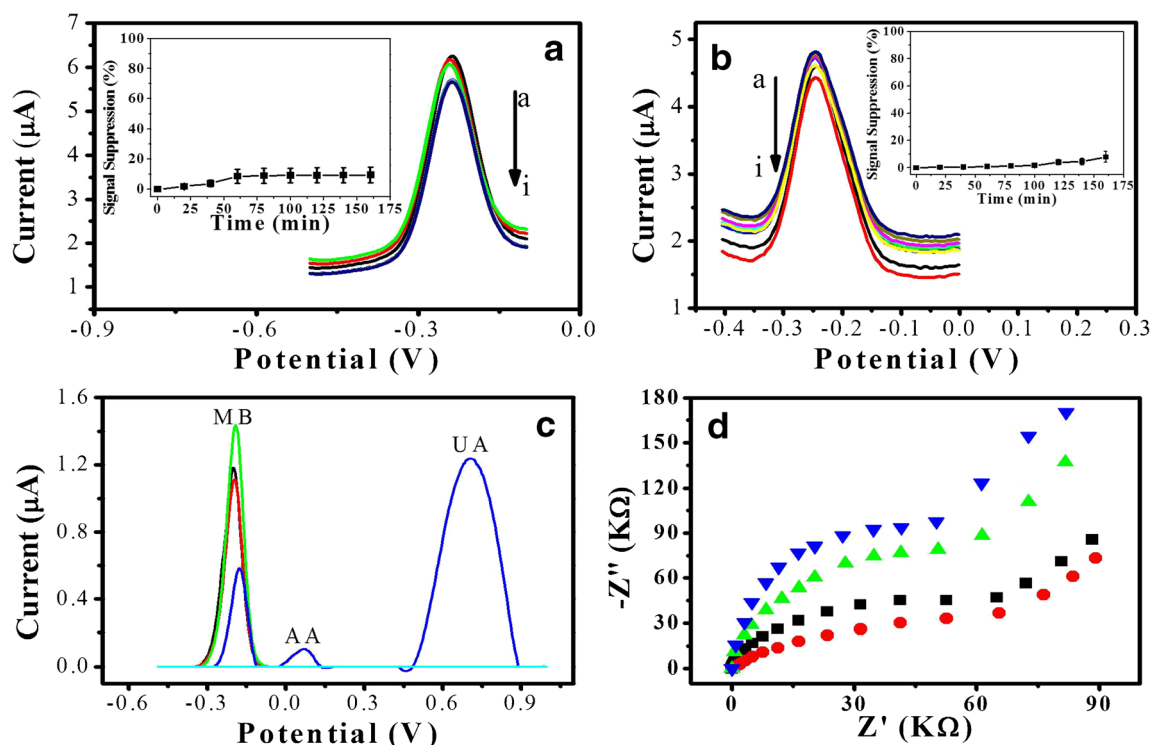


Fig. 2 **a** Square wave voltammetry of the PSA aptasensor stabilization over time (a–i: 0, 20, 40, 60, 80, 100, 120, 140, and 160 min) at potential range from 0.0 to -0.5 V, at 40 mV amplitude, and frequency 60 Hz. **b** Square wave voltammetry of the VEGF aptasensor stabilization over time (a–i: 0, 20, 40, 60, 80, 100, 120, 140, and 160 min) at potential range from 0.0 to -0.5 V, at 40 mV amplitude, and frequency 60 Hz, in 10 mM PBS buffer (pH 7.4). **c** Square wave voltammetry of step-by-step modification of aptasensor at potential range from 1.0 to -0.5 V, at 40 mV amplitude,

and frequency 60 Hz, bare gold electrode (blue line) aptamer immobilization (green line), surface blocking by MCH (black line), adding the filter (red line), adding recombinant protein and interfering compounds (AA and UA) (dark blue line). **d** Nyquist plots for step-by-step aptasensor assembling; bare gold surface (*), aptamer immobilization (•), MCH backfilling (▲) and binding of recombinant protein (▼). Frequency intervals were from 0.001 to 10,000 Hz

signal loss was checked through SWV and converted into signal suppression (SS) percentage. All measurements were carried out in triplicate and the limit of detection (LOD) was calculated through linear regression by using the standard deviation of the y-intercept ($LOD = 3\sigma/Slope$).

Electrochemical detection of the PSA and VEGF released by prostate cells

The electrochemical measurements applied to human prostate cells followed the same procedures described above, with minor modifications. Therefore, the electrochemical cell containing VEGF and PSA aptamers was kept under 5% CO_2 , 95% air humidity atmosphere, at 37 °C. The millipore membrane was added on the top of working electrode with a dual purpose, to be a barrier and to provide substrate for cells attachment without harming aptamer surface. It was done to avoid signal disruption due to cell adsorption over the working electrode modified by the aptamers. The SWV measurements were taken every 20 min, for 3 h, after cell incubation (Scheme 1).

Results and discussion

Optimization and characterization of aptasensor

The gold-coated silicon wafer surface was investigated through SEM and EDS, in order to assure the formation of a well-dispersed gold layer of dual purpose, namely acting as working electrode, and anchoring the thiolated aptamer on the surface. Figure 1a shows a bare silicon wafer, partially coated with gold, to evidence the formation of a uniform thin gold layer on the top of the surface; however, without any open space or gold agglomerate. Moreover, Fig. 1b represents the EDS scan of the surface, which was performed to assure the presence of gold atoms; therefore, it is possible verifying the unique set of gold and silicon peaks in the electromagnetic emission spectrum [28]. Figure 1c shows a typical cyclic voltammogram of gold surfaces presenting cathodic peak at +1.45 V, and anodic peak at +0.8 V; the 25 cycles (black lines) indicate enhanced electron transfer after gold layer deposition on top of silicon wafer with

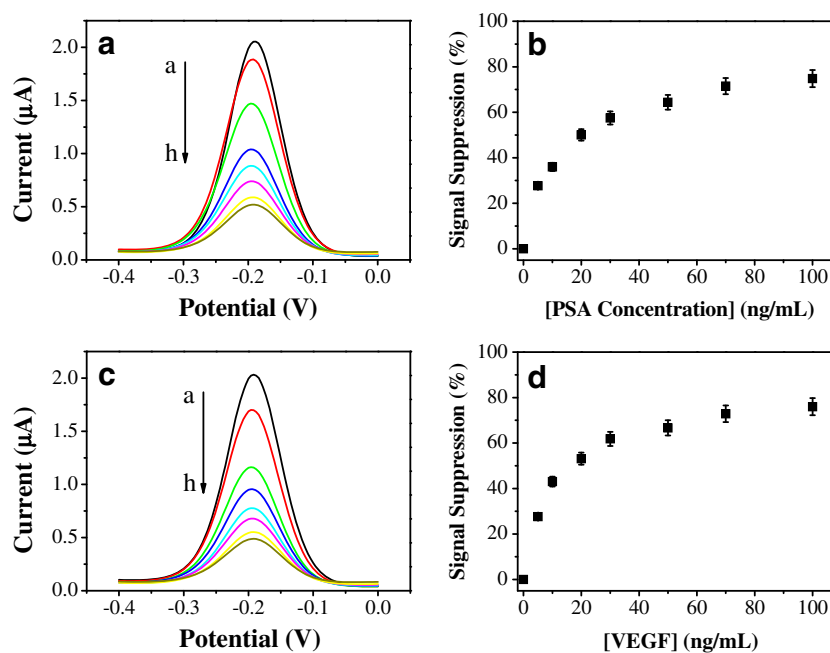


Fig. 3 **a** Square wave voltammetry plot of the PSA aptasensor at potential range 0.0 to -0.5 V, at 40 mV amplitude, and frequency 60 Hz—as PSA concentration function (a–i: 0, 5, 10, 20, 30, 50, 70, and 100 ng/mL), in 10 mM PBS buffer (pH 7.4). **b** Calibration plot of the PSA aptasensor showing signal suppression rate in signal loss percentage and SWV peak current as the function of several PSA

concentrations. **c** Square wave voltammetry plot of the VEGF aptasensor at potential range 0.0 to -0.5 V, at 40 mV amplitude, and frequency 60 Hz—as VEGF concentration function (a–i: 0, 5, 10, 20, 30, 50, 70, and 100 ng/mL). **d** Calibration plot of the VEGF aptasensor showing signal suppression rate in signal loss percentage of the SWV peak current as the function of several VEGF concentrations

high stability, which can be used as working electrode, in contrast to bare Si surface (red line) [29].

The aptamer immobilization on the top of the gold-coated silicon wafer was accomplished through surface coordinated chemistry, which generated well-defined surface patterns by using thiols linkers attached to the gold layers in order to form self-assembled monolayers (SAMs) [29]. Real time monitoring of layer formation by SPR technique revealed a well disperse aptamer surface with density of 6.6 ng/mm^2 [30]. Subsequently, the surface was passivated through the backfilling technique, with MCH, which is a well-known methodology to work with thiolated DNA sensor surfaces [31].

The electrochemical behavior of the aptamer biosensor was analyzed through square wave voltammetry (SWV), using MB as redox indicator. The MB redox tag was chosen due to the possibility of anchoring it on the aptamers hairpin structure; it is also used in a wide range of aptamers to detect several protein and cytokine types, as well as other biomarker types [32–34]. The aptamer surface stability was achieved by measuring SWV in buffer for 2.5 h, before detecting the aptasensor to target the proteins (PSA and VEGF). Figure 2a, b represents the PSA and VEGF stability in the herein developed sensor over time. The background signal starts to stabilize after 1 h measurement, it shows lower signal suppression (less than 10% signal loss), as well as stability comparable to that of other electrochemical aptamer biosensor types [14, 32, 35].

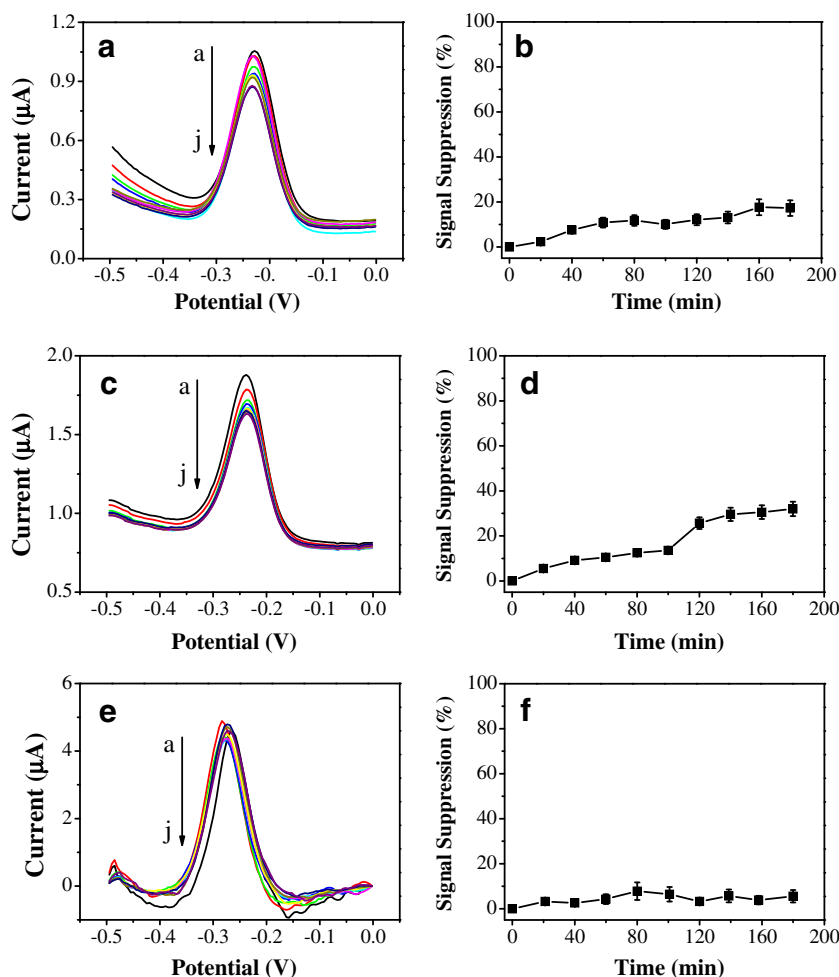
Moreover, SWV, EIS and were done over step by step assembling of the aptasensor as shown in Fig. 2c. The MB peak remained constant on every step, even the addition of the filter did not cause electrochemical hindrance or disruption of the signal. In addition, to verify interfering compounds species, 100 mM of AA and UA was added and there was no competitive peak over MB peak range.

EIS was performed to evaluate charge transfer resistance. Figure 2d shows the Nyquist plots of impedance, the semicircle diameter can be related with the charge transfer resistance (R_{ct}) at the electrode surface. Figure 2d shows the EIS spectra on a step-by-step assembling of the aptasensor; the R_{ct} was 17 $k\Omega$ for bare Au surface (black squares). After aptamer immobilization, the resistance increased to 31 $k\Omega$ (red circles), consequently adding MCH and recombinant protein also increased the resistance (56 $k\Omega$ and 83 $k\Omega$, respectively) which validate the formation of each layer of the aptamer-based biosensor.

PSA and VEGF detection and monitoring

The calibration curve was obtained to quantify the limit of detection and the linear detection range of PSA and VEGF after stability optimization; therefore, the aptasensor was challenged in several target protein concentrations (from 5 to 100 ng/mL). Figure 3a represents the SWV graph of the PSA calibration curve, and Fig. 3b plots signal losses caused

Fig. 4 **a** Square wave voltammetry plot of the PSA released by the RWPE-1 line at potential range from 0.0 to -0.5 V, at 40 mV amplitude, and frequency 60 Hz over time in RPMI media. **b** Signal suppression rate in signal loss percentage of the SWV peak current as the function of several PSA released by the RWPE-1 line. **c** Square wave voltammetry plot of the PSA released by the LNCaP line at potential range from 0.0 to -0.5 V, at 40 mV amplitude, and frequency 60 Hz over time RPMI media. **d** Signal suppression rate in signal loss percentage of the SWV peak current as the function of several PSA released by the LNCaP line. **e** Square wave voltammetry plot of the PSA released by the PC3 line at potential range from 0.0 to -0.5 V, at 40 mV amplitude, and frequency 60 Hz over time RPMI media. **f** Signal suppression rate in signal loss percentage of the SWV peak current as the function of several PSA released by the PC3 line



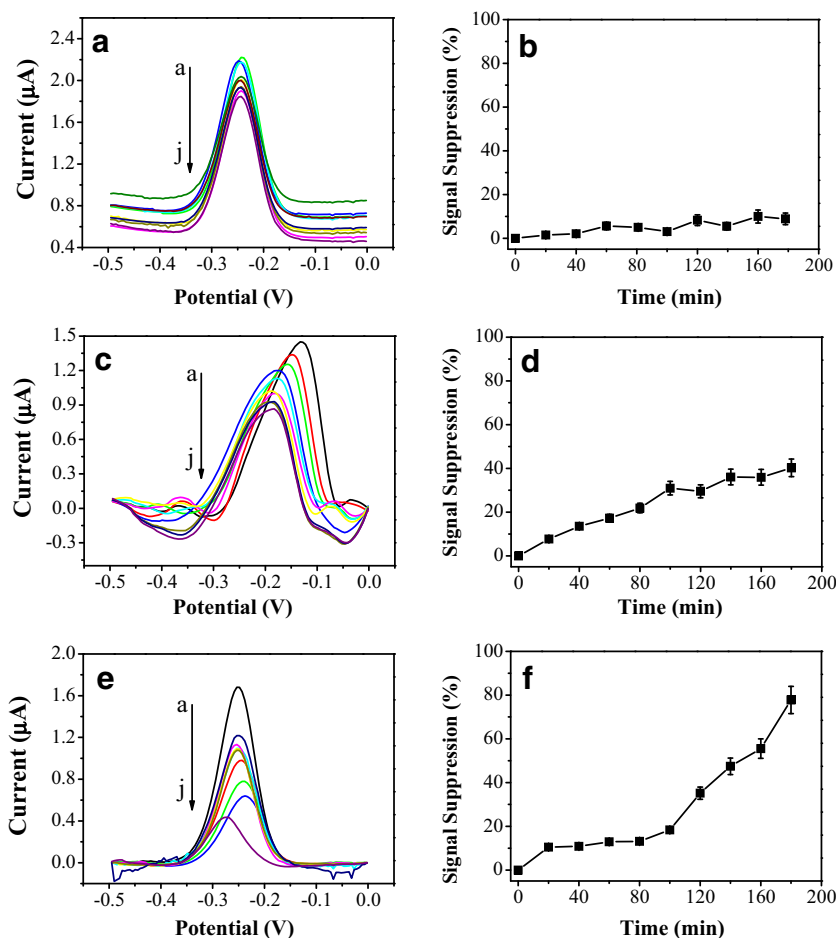
by the PSA binding to the aptasensor, according to the following calculation: $\Delta I = I_{pb} - I_{pa}$ (ΔI = change in current, I_{pb} = peak current before protein incubation and I_{pa} = peak current after protein incubation); these losses were converted into signal loss (SS) percentage. The PSA signal suppression (Fig. 3b) linearly increased due to the PSA concentration; wherein: $SS = 0.61 + 1.9 \times (R^2 = 0.989)$, and the detection limit was estimated to be 1.1 ng/mL—with linear range of 0–100 ng/mL. The present aptasensor can be used to detect PSA in clinical samples, because its PSA range in PCa is higher than 4 mg/mL [10]. The repeatability was expressed as the relative standard deviation (RSD 4.2%) value of the signal suppression for five injections of the same concentration of PSA protein at different times. These results reveal that the aptasensor has higher activity with higher affinity to PSA.

The VEGF was analyzed through the same protocol, in addition to the PSA calibration curve. Figure 3c shows the SWV of the VEGF calibration curve, which evidences changes in the peak current in every challenge set in each of the tested proteins. Figure 3d shows linear SS increasing at VEGF concentration wherein $SS = 0.23 + 2.05 \times (R^2 = 0.986)$, and limit of detection was calculated at 0.32 ng/mL. The

repeatability calculated 5.2% value of the signal suppression for five injections of the same concentration of VEGF protein at different times. These results are comparable to other biosensor types used to detect VEGF and PSA; they can be used to monitor the protein released by prostate cells (normal and cancerous) [14].

The literature provides a wide range of studies aimed at developing aptamers to target VEGF and PSA; however, few studies have actually focused on using aptamers to detect the PSA and VEGF released by cells and this is of utmost importance due to the need to understand protein released patterns by different types of cells which can be correlated with cancer aggressiveness [8, 14, 36]. The PSA and VEGF release dynamics may change depending on the used prostate cell type. Three (3) cell lines were chosen, a control line (normal prostate cells, RWPE-1), an androgen-sensitive human prostate cancer cell (LNCaP), and a more aggressive androgen-independent human prostate cancer cell (PC-3) [37]. The optimization of the aptasensor stability was performed to make sure about the acquisition of optimal data through fast experiments in order to create a robust biosensor to be used for clinical diagnostics. Thus, cells and aptamers

Fig. 5 **a** Square wave voltammetry plot of the VEGF released by the RWPE-1 line at potential range from 0.0 to -0.5 V, at 40 mV amplitude, and frequency 60 Hz over time RPMI media. **b** Signal suppression rate in signal loss percentage of the SWV peak current as the function of several VEGF released by the RWPE-1 line. **c** Square wave voltammetry plot of the VEGF released by the LNCaP line at potential range from 0.0 to -0.5 V, at 40 mV amplitude, and frequency 60 Hz over time RPMI media. **d** Signal suppression rate in signal loss percentage of the SWV peak current as the function of several VEGF released by the LNCaP line. **e** Square wave voltammetry plot of the VEGF released by the PC3 line at potential range from 0.0 to -0.5 V, at 40 mV amplitude, and frequency 60 Hz over time RPMI media. **f** Signal suppression rate in signal loss percentage of the SWV peak current as the function of several VEGF released by the PC3 line



were left to rest for 1 h in order to stabilize and reduce the background signal from electrochemical experiments, before the SWV measurements from cells were taken.

The PSA monitoring patterns are shown in Fig. 4. The PSA produced through RWPE-1 (Fig. 4a, b) was approximately 2 ng/mL at the end of the experiment; it was comparable to the PSA levels presented by healthy patients. The PSA was overexpressed as LNCaP, because it presented values close to 5 ng/mL at the end of the experiment (Fig. 4c, d). On the other hand, the PC3 line (Fig. 4e, f) showed almost no PSA production. The detection of PSA by aptasensor is in line with cells lineage type, due to the androgen dependence and active androgen receptor of LNCaP, an overexpressed PSA released was verified [38, 39]. For PC3 cells a zero production of PSA was achieved, since this cell type had a lack in PSA gene expression [40, 41]. Accordingly, the current findings are in compliance to the PSA release dynamics, and it can be associated with tumor aggressiveness and gene alterations. The LNCaP cell lines were able to produce larger PSA amounts in RPMI, and consequently, to lead to the wide range of PSA concentrations described in the literature (from 0.1 to 110 ng/mL) [42, 43]. In addition, the multifarious results concerning the PSA released by LNCaP meet experiments conducted in vivo, because of the acute and

chronic stimuli that may modulate the PSA expression by cancer cells [44, 45]. Moreover, the PC3 cells usually do not produce PSA, fact that can be associated with tumor aggressiveness due to cells' androgen-independence to proliferate [46, 47].

The VEGF monitoring patterns are shown in Fig. 5 in parallel to the PSA detection. The monitoring of VEGF from prostate cells can give new insights about targeting of different PCa, and it may expand the range of biomarkers used in early prostate cancer diagnostics; besides, it can be related to tumor aggressiveness [48, 49]. The RWPE-1 (Fig. 5a, b) showed zero VEGF production and SS comparable to the background signal throughout the whole experiment. On the other hand, LNCaP (Fig. 5c, d) and PC3 (Fig. 5e, f) have shown an overexpressed VEGF production and higher SS value at the end of the experiment (5 ng/mL for LNCaP and 30 ng/mL for PC3). The higher VEGF production in PC3 is explained by the metastatic aggressiveness of this line, which is able to spread all over the human body; whereas LNCaP is a less aggressive PCa type [50, 51]. The VEGF release dynamics shown in the present study meet the results described in the literature, namely higher VEGF expressions are related to patients with metastatic prostate cancer [52, 53].

Conclusions

The present study addresses a new aptamer-based biosensor capable of monitoring the PSA and VEGF released from prostate cells (normal and cancerous) through a biosensor based on aptamers on the top of gold electrodes. The PSA and VEGF detection limits were 0.08 ng/mL and 0.15 ng/mL, respectively, at linear range up to 100 ng/mL. In addition, the herein developed aptasensor was able to verify, at accurate and robust response, the patterns of the PSA and VEGF released by different cell lines (RWPE-1, LNCaP and PC3); it is the first aptasensor type used to access the patterns of protein production and release presented by PCa. This biosensor can be a useful clinical diagnosis instrument to detect initial PCa stages in the near future.

Acknowledgments The authors thank FAPESP (2016/15919-8), CAPES and CNPq, Brazil, for the grants and the financial support to this work.

Compliance with ethical standards

Conflict of interest The authors declare that they have no conflict of interest.

References

- Stewart BW, Wild CP. World cancer report. In: World Health Organization. International Agency for Research on Cancer. 2014. <http://publications.iarc.fr/Non-Series-Publications/World-Cancer-Reports/World-Cancer-Report-2014>. Accessed 20 Jul 2017.
- Schröder FH, Hugosson J, Roobol MJ, Tammela TLJ, Ciatto S, Nelen V, et al. Screening and prostate-cancer mortality in a randomized European study. *New Engl J Med*. 2009;360:1320–8.
- Catalona WJ, Richie JP, Ahmann FR, Hudson MA, Scardino PT, Flanigan RC, et al. Comparison of digital rectal examination and serum prostate specific antigen in the early detection of prostate cancer: results of a multicenter clinical trial of 6,630 men. *J Urol*. 1994;151:1283–90.
- Catalona WJ, Smith DS, Omstein DK. Prostate cancer detection in men with serum PSA concentrations of 2.6 to 4.0 ng/mL and benign prostate examination: enhancement of specificity with free PSA measurements. *JAMA*. 1997;277:1452–5.
- Mitchell PS, Parkin RK, Kroh EM, Fritz BR, Wyman SK, Pogosova-Agadjanyan EL, et al. Circulating microRNAs as stable blood-based markers for cancer detection. *Proc Natl Acad Sci*. 2008;105:10513–8.
- Jolly P, Formisano N, Estrela P. DNA aptamer-based detection of prostate cancer. *Chem Pap*. 2015;69:77–89.
- Pentyala S, Pentyala TWS, Muller J, Pfail J, Parmar S, Helguero CG, et al. Prostate cancer markers: an update. *Biomed Rep*. 2016;4:263–8.
- Parra-Cabrera C, Samitier J, Homs-Corbera A. Multiple biomarkers biosensor with just-in-time functionalization: application to prostate cancer detection. *Biosens Bioelectron*. 2016;77:1192–200.
- Ung JO, Richie JP, Chen MH, Renshaw AA, D'Amico AV. Evolution of the presentation and pathologic and biochemical outcomes after radical prostatectomy for patients with clinically localized prostate cancer diagnosed during the PSA era. *Urology*. 2002;60:458–63.
- Ushaa SM, Madhavalatha M, Rao GM. Design and analysis of nanowire sensor array for prostate cancer detection. *Int J Nano Biomater*. 2011;3:239–55.
- Klein LT, Lowe FC. The effects of prostatic manipulation on prostate-specific antigen levels. *Urol Clin North Am*. 1997;24:293–7.
- Stephan C, Cammann H, Meyer HA, Lein M, Jung K. PSA and new biomarkers within multivariate models to improve early detection of prostate cancer. *Cancer Lett*. 2007;249:18–29.
- Stamey TA, Caldwell M, McNeal JE, Nolley R, Hemenez M, Downs J. The prostate specific antigen era in the United States is over for prostate cancer: what happened in the last 20 years? *J Urol*. 2004;172:1297–301.
- Pan LH, Kuo SH, Lin TY, Lin CW, Fang PY, Yang HW. An electrochemical biosensor to simultaneously detect VEGF and PSA for early prostate cancer diagnosis based on graphene oxide/ssDNA/PLLA nanoparticles. *Biosens Bioelectron*. 2017;89:598–605.
- Gerber HP, Vu TH, Ryan AM, Kowalski J, Werb Z, Ferrara N. VEGF couples hypertrophic cartilage remodeling, ossification and angiogenesis during endochondral bone formation. *Nat Med*. 1999;5:623–8.
- Duffy AM, Bouchier-Hayes DJ, Harmey JH. Vascular endothelial growth factor (VEGF) and its role in non-endothelial cells: autocrine signalling by VEGF. *VEGF and Cancer*. 2004;133–44.
- Cooper M, Dimitria V, Sherif Y, Steven AS, Alison JC, Bishoy R, et al. Increased renal expression of vascular endothelial growth factor (VEGF) and its receptor VEGFR-2 in experimental diabetes. *Diabetes*. 1999;48:2229–39.
- Ohta Y, Endo Y, Tanaka M, Shimizu J, Oda M, Hayashi Y, et al. Significance of vascular endothelial growth factor messenger RNA expression in primary lung cancer. *Clin Cancer Res*. 1996;2:1411–6.
- Takahashi Y, Kitadai Y, Bucana CD, Cleary KR, Ellis LM. Expression of vascular endothelial growth factor and its receptor, KDR, correlates with vascularity, metastasis, and proliferation of human colon cancer. *Cancer Res*. 1995;55:3964–8.
- Yamamoto Y, Toi M, Kondo S, Matsumoto T, Suzuki H, Kitamura M, et al. Concentrations of vascular endothelial growth factor in the sera of normal controls and cancer patients. *Clin Cancer Res*. 1996;2:821–6.
- Zhang B, Liu B, Chen G, Tang D. Competitive-type displacement reaction for direct potentiometric detection of low-abundance protein. *Biosens Bioelectron*. 2014;53:465–71.
- Zhang Y, Chen Y, Han D, Ocsosy I, Tan W. Aptamers selected by cell-SELEX for application in cancer studies. *Bioanalysis*. 2010;2:907–18.
- Poma A, Brahmabhatt H, Pendergraff HM, Watts JK, Turner NW. Generation of novel hybrid aptamer–molecularly imprinted polymeric nanoparticles. *Adv Mater*. 2015;27:750–8.
- Souza AG, Marangoni K, Fujimura PT, Alves PT, Silva MJ, Bastos VAF, et al. 3D Cell-SELEX: development of RNA aptamers as molecular probes for PC-3 tumor cell line. *Exp Cell Res*. 2016;341:147–56.
- Ohuchi S. Cell-SELEX technology. *Biores Open Access*. 2012;1:265–72.
- Jayasena SD. Aptamers: an emerging class of molecules that rival antibodies in diagnostics. *Clin Chem*. 1999;45:1628–50.
- Liu Y, Zhou Q, Revzin A. An aptasensor for electrochemical detection of tumor necrosis factor in human blood. *Analyst*. 2013;138:4321–6.
- Wang R, Liu J, Liu P, Bi X, Yan X, Wang W, et al. Dispersing Pt atoms onto nanoporous gold for high performance direct formic acid fuel cells. *Chem Sci*. 2014;5:403–9.

29. Wahl A, Dawson K, Sassiati N, Quinn AJ, O'Riordan A. Nanomolar trace metal analysis of copper at gold microband arrays. *J Phys: Conf Ser.* 2011;307:012061.
30. Karpik AE, Crulhas BP, Rodrigues CB, Castro GR, Pedrosa VA. Aptamer-based biosensor developed to monitor MUC1 released by prostate cancer cells. *Electroanalysis.* 2017;29:1–9.
31. Basso CR, de Camargo Tozato C, Ribeiro MCM, Junior JPA, Pedrosa VA. A immunosensor for the diagnosis of canine distemper virus infection using SPR and EIS. *Anal Methods.* 2013;5:5089–95.
32. Gong P, Levicky R. DNA surface hybridization regimes. *Proc Natl Acad Sci U S A.* 2008;105:5301–6.
33. Liu Y, Tuleuova N, Ramanculov E, Revzin A. Aptamer-based electrochemical biosensor for interferon gamma detection. *Anal Chem.* 2010;82:8131–6.
34. Xiao Y, Lubin AA, Heeger AJ, Plaxco KW. Label-free electronic detection of thrombin in blood serum by using an aptamer-based sensor. *Angew Chem.* 2005;117:5592–5.
35. Xiao Y, Piorek BD, Plaxco KW, Heeger AJ. A reagentless signal-on architecture for electronic, aptamer-based sensors via target-induced strand displacement. *J Am Chem Soc.* 2005;127:17990–1.
36. Kido S, Kitadai Y, Hattori N, Haruma K, Kido T, Ohta M, et al. Interleukin 8 and vascular endothelial growth factor—prognostic factors in human gastric carcinomas? *Eur J Cancer.* 2001;37:1482–7.
37. Duque JLF, Loughlin KR, Adam RM, Kantoff PW, Zurakowski D, Freeman MR. Plasma levels of vascular endothelial growth factor are increased in patients with metastatic prostate cancer. *Urology.* 1999;54:523–7.
38. Kampa M, Papakonstanti EA, Hatzoglou A, Stathopoulos EN, Stournaras C, Castanas E. The human prostate cancer cell line LNCaP bears functional membrane testosterone receptors that increase PSA secretion and modify actin cytoskeleton. *FASEB J.* 2002;16:1429–31.
39. Nicotera TM, Schuster DP, Bourhim M, Chadha K, Klaich G, Corral DA. Regulation of PSA secretion and survival signaling by calcium-independent phospholipase A2 β in prostate cancer cells. *Prostate.* 2009;69:1270–80.
40. Kaighn ME, Narayan KS, Ohnuki Y, Lechner JF, Jones LW. Establishment and characterization of a human prostatic carcinoma cell line (PC-3). *Investig Urol.* 1979;17:16–23.
41. Russell PJ, Kingsley EA. Human prostate cancer cell lines. *Prostate Cancer Methods and Protocols.* 2003;81:21–39.
42. Zhu Y-S, Cai L-Q, You X, Cordero JJ, Huang Y, Imperato-McGinley J. Androgen-induced prostate-specific antigen gene expression is mediated via dihydrotestosterone in LNCaP cells. *J Androl.* 2003;24:681–7.
43. Fujii Y, Kawakami S, Okada Y, Kageyama Y, Kihara K. Regulation of prostate-specific antigen by activin A in prostate cancer LNCaP cells. *Am J Physiol Endocrinol Metab.* 2004;286:927–31.
44. Gkonos PJ, Kwok CK, Block NL, Roos BA. Identification of the human seminal TRH-like peptide pGlu-Phe-Pro-NH₂ in normal human prostate. *Peptides.* 1994;15:1281–3.
45. Lee C, Sutkowski DM, Sensibar JA, Zelner D, Kim I, Amsel I, et al. Regulation of proliferation and production of prostate-specific antigen in androgen-sensitive prostatic cancer cells, LNCaP, by dihydrotestosterone. *Endocrinology.* 1995;136:796–803.
46. Nosratollah Z, Habib O, Behrangh A. Association between steroid hormone receptors and PSA gene expression in breast cancer cell lines. *Afr J Biotechnol.* 2005;4:1415–20.
47. Tsui K-H, Feng T-H, Chung L-C, Chao C-H, Chang P-L, Juang H-H. Prostate specific antigen gene expression in androgen insensitive prostate carcinoma subculture cell line. *Anticancer Res.* 2008;28:1969–76.
48. König JE, Senge T, Allhoff EP, König W. Analysis of the inflammatory network in benign prostate hyperplasia and prostate cancer. *Prostate.* 2004;58:121–9.
49. Martin DB, Gifford DR, Wright ME, Keller A, Yi E, Goodlett DR, et al. Quantitative proteomic analysis of proteins released by neoplastic prostate epithelium. *Cancer Res.* 2004;64:347–55.
50. Lin CW, Wei KC, Liao SS, Huang CY, Sun CL, Wu PJ, et al. A reusable magnetic graphene oxide-modified biosensor for vascular endothelial growth factor detection in cancer diagnosis. *Biosens Bioelectron.* 2015;67:431–7.
51. Ferrer FA, Miller LJ, Andrawis RI, Kurtzman SH, Albertsen PC, Laudone VP, et al. Vascular endothelial growth factor (VEGF) expression in human prostate cancer: in situ and in vitro expression of VEGF by human prostate cancer cells. *J Urol.* 1997;157:2329–33.
52. Ferrara N, Davis-Smyth T. The biology of vascular endothelial growth factor. *Endocr Rev.* 1997;18:4–25.
53. Woollard DJ, Opeskin K, Coso S, Wu D, Baldwin ME, Williams ED. Differential expression of VEGF ligands and receptors in prostate cancer. *Prostate.* 2013;73:563–72.